Molecular Weight Dependence of Glassy Dynamics in Linear Polymers Revisited

J. Hintermeyer, A. Herrmann, R. Kahlau, C. Goiceanu, and E. A. Rössler*

Experimentalphysik II, Universität Bayreuth, 95440 Bayreuth, Germany

Received March 19, 2008

ABSTRACT: Dielectric spectra of a series of polydimethylsiloxanes and polystyrenes were measured covering a wide range of molecular weights M including the monomeric limit. From spectral analysis the time constants $\tau_\alpha(T)$ of the segmental dynamics are extracted, allowing determination of the glass-transition temperatures $T_g(M)$ and $\tau_\alpha(M)$ as well as the parameters $D(M)$ and $T_0(M)$, respectively, $\Delta(M) = T_g - T_0$, of the Vogel−Fulcher−Tammann equation. In addition, we analyzed fragility $m(M)$ including here also data on polybutadiene. It turns out that all the quantities show particularities as a function of M which are not explained by common wisdom. $T_g(M)$ as well as $T_0(M)$ data reveal a noncontinuous M dependence with three distinct regimes which may become plausible when comparing our results with rheological and NMR data. We attribute the three regimes to simple liquid, Rouse, and entanglement dynamics, i.e., $T_g(M)$ and $T_0(M)$ traces show kinks at the Rouse unit M_R and entanglement molecular weight M_e. Fragility $m(M)$ shows only one kink at M_e. This fact can be explained by the behavior of $\Delta(M)$, which increases with M in the simple liquid regime but saturates already at M_R; a similar behavior is observed for the exponential prefactor $\tau_0(M)$. We conclude that polymer dynamics specifically modify glassy dynamics.

1. Introduction

It is a well-established fact that the glass-transition temperature T_g of linear polymers increases with molecular weight M and saturates at high M. The quantity T_g may be taken as a measure of the temperature scale, indicating the strong slowing down of segmental dynamics characteristic of glassy dynamics. Conventionally, T_g is defined as the temperature for which the segmental time scale becomes $\tau_s = 100$ s. Likewise, T_g may be determined by a DSC experiment with a cooling rate of 10 K/min. Though often monitored in polymers, the glass transition is a generally observed phenomenon also appearing in simple liquids. The controlling process is called the structural relaxation or α-process. It determines the relaxation of nonpolymeric liquids at longest times. In polymeric systems relaxations on even longer time scales appear, reflecting the collective response due to connectivity and entanglement. Still, the glass transition drives the temperature dependence of the collective chain dynamics, and the segmental time scale τ_s may be identified with the time constant τ_α of the α-process.

It is an important question whether polymer dynamics modify glassy dynamics. Moreover, regarding when does a molecule become a polymer,[1,2] a final answer is still missing. Concerning the collective dynamics of linear polymers, depending on M they may be described by either the Rouse model below the entanglement threshold M_e or the reptation model ($M > M_e$), where M_e denotes the molecular weight between entanglements.[3] Starting from a monomer and increasing the chain length, one expects first the Rouse dynamics to set in at the molecular weight M_R of the Rouse unit followed thereafter by the reptation dynamics at $M > M_e$. Often, M_e is determined from rheological experiments and known for many polymers. In contrast, not much is known about the molecular weight at which first Rouse modes set in and thus defines the crossover from a simple liquid to a polymer melt.

Plenty of data demonstrate the saturation behavior of $T_g(M)$ (see section F). In most cases a continuous increase of $T_g(M)$ is assumed; neither M_e nor M_R are believed to be directly reflected in $T_g(M)$. Instead, $T_g(M)$ expressions are discussed, e.g., accounting for the introduction of additional free volume due to the presence of end groups[4] or $T_g(M)$ is related to the establishment of Gaussian chain dynamics.[1] Reporting results from dielectric spectroscopy (DS) and fast field cycling (FFC) NMR, this view has been recently challenged.[5,6] In the case of 1,4-polybutadiene (PB), we reported a discontinuous behavior of $T_g(M)$ showing kinks at M_R and M_e. Actually, such a discontinuous behavior was already published long time ago[7,8] and found entry into textbooks by Cowie[9,10] and Sperling;[11] however, it appears that this knowledge got lost in the third edition.[12] Many of the $T_g(M)$ data in the literature show strong scatter and do not cover the full M range needed to monitor the crossover from monomeric glass former to high M polymer. Indeed, it is an experimental challenge to measure "polymers" with low M as crystallization usually interferes.

It is the purpose of this publication to present high-precision DS data for polydimethlysiloxane (PDMS) and polystyrene (PS) covering a wide range of molecular weights. In addition to determining $T_g(M)$ from the dielectric spectra we will also investigate the extent of non-Arrhenius temperature dependence of the segmental time constants $\tau_\alpha(T)$ via the M dependence of the parameters of the Vogel−Fulcher−Tammann (VFT) equation. Moreover, the fragility index m will be discussed as a function of M, a topic recently addressed by several authors.[13−18] Here, we include also an analysis of recently published dielectric data of polybutadiene (PB).[6] Finally, we will inspect the change of the spectral shape of α-relaxation when going from the limit of a monomeric glass former to a high molecular weight system. Together with reinspecting literature data our works suggest that indeed $T_g(M)$ traces reveal two kinks, and it may be worthwhile to associate these crossovers with the onset of Rouse and reptation dynamics at M_R and M_e, respectively.

2. Experimental Section

Dielectric spectra were measured by applying an Alpha-A spectrometer from Novocontrol. A series of polydimethylsiloxanes (PDMS) with weight-averaged $M = M_w$ values (in g/mol) in the range from 311−232 000 and polydispersity $M_w/M_n = 1.0-1.43$ and of polystyrene (PS) with weight-averaged M_w values in the

* To whom correspondence should be addressed. E-mail: ernst.roessler@uni-bayreuth.de.

10.1021/ma8016794 CCC: $40.75
Published on Web 11/04/2008

Table 1. Investigated Polydimethylsiloxane (PDMS) Samples: Molecular Weight M_w, Polydispersity M_w/M_n, Glass-Transition Temperature T_g Determined from Analyzing Dielectric Spectra, and Vogel−Fulcher−Tammann Temperature T_0

polydimethylsiloxane	M_w [g/mol]	M_w/M_n	T_g [K]	T_0 [K]
PDMS311	311	1	126.3	105.4
PDMS860	860	1.41	133.6	112.6
PDMS1600	1600	1.37	138.2	118.3
PDMS2490	2490	1.4	139.9	119.3
PDMS3510	3510	1.32	141.5	120.4
PDMS4560	4560	1.43	142.4	121.9
PDMS5940	5940	1.15	143.0	122.4
PDMS11000	11 000	1.05	144.0	123.6
PDMS21600	21 600	1.04	144.2	123.7
PDMS41400	41 400	1.03	144.5	123.9
PDMS128000	128 000	1.13	144.4	123.9
PDMS232000	232 000	1.06	144.6	124.1

Table 2. Investigated Polystyrene (PS) Samples: Molecular Weight M_w, Polydispersity M_w/M_n, Glass-Transition Temperature T_g Determined from Analyzing Dielectric Spectra, and Vogel−Fulcher−Tammann Temperature T_0

polystyrene	M_w [g/mol]	M_w/M_n	T_g [K]	T_0 [K]
PS106	106	1.0	114.7	84.0
PS162	162	1.0	138.9	102.0
PS370	370	1.0	231.9	190.0
PS690	690	1.09	261.4	218.0
PS1350	1350	1.05	314.2	268.0
PS3250	3250	1.05	347.0	300.0
PS8900	8900	1.03	356.9	311.5
PS19100	19 100	1.03	367.9	320.8
PS33500	33 500	1.03	369.0	323.2
PS96000	96 000	1.03	372.6	326.5
PS243000	243 000	1.03	373.3	327
PS546000	546 000	1.02	372.0	325

Table 3. Investigated 1,4-Polybutadiene (PB) Samples: Molecular Weight M_w, Polydispersity M_w/M_n, Glass-Transition Temperature T_g Determined from Analyzing Dielectric Spectra, and Vogel−Fulcher−Tammann Temperature T_0[6]

polybutadiene	M_w [g/mol]	M_w/M_n	T_g [K]	T_0 [K]
PB355	355	1	140.9	112.5
PB466	466	1.07	161.2	131.0
PB575	575	1.07	162.1	132.0
PB777	777	1.06	165.3	134.5
PB1450	1450	1.07	170.7	141.0
PB2020	2020	1.07	173.6	144.0
PB2760	2760	1.05	174.5	143.5
PB4600	4600	1.03	174.0	144.0
PB19900	19 900	1.03	175.3	143.5
PB35300	35 300	1.03	174.5	144.1
PB87000	87 000	1.01	174.4	143.5

range 106−546 000 with polydispersity $M_w/M_n = 1.0-1.1$ were measured. The dielectric data of polybutadiene (PB) were published before.[5,6,19] All polymers were purchased from Polymer Standards Service (Germany). The polymers bear the following end groups: PDMS, *n*-butyl and trimethylsilan; PS as well as PB, *sec*-butyl and H. Tables 1 (PDMS), 2 (PS), and 3 (PB) list the molecular weight, polydispersity, and determined T_g as well as T_0 (from the Vogel−Fulcher−Tammann equation, eq 2) values of the samples. For PS we were able to monitor the glass transition of its monomeric liquid ethyl benzene. The microstructure of the PB samples was determined by high-resolution ^{13}C NMR,[19] and the amount of vinyl content was found to be 6−8% above $M = 10^4$ and increases up to 20% (at $M = 800$) below. The cis/trans ratio was around 4/5. The polymers are of type B[20] as they do not show any discernible dielectric normal mode. Thus, DS probes the segmental respectively glassy dynamics only. In order to avoid crystallization, in particular for all PDMS samples and also for all low M samples of PB and PS, the filled dielectric cell was quenched below T_g and then slowly heated. For temperatures close to T_g, prior to starting a measurement the sample was kept sufficiently long at the selected temperature to guarantee equilibrium. For each sample we tried to reach time constants close to or even above 100 s as we define T_g via the condition $\tau_\alpha(T_g) = 100$ s. In order to check whether equilibrium in the polymer melt is always maintained while measuring dielectric spectra down to 10^{-3} Hz we inspected $T_g(M)$ fixed by the condition $\tau(T_g) = 1$ s, but no systematic difference is observed. Thus, we conclude that the waiting time applied for lowest temperature was sufficient to guarantee equilibrium.

The dielectric spectra were interpolated by applying an extension of the generalized gamma distribution (GGE) of relaxation times. This function is discussed in detail in refs 21 and 22. Here, it suffices to note that the GGE function is able to interpolate both the α-peak and the so-called excess wing on the high-frequency side of the α-peak and as demonstrated below allows also interpolating all the spectra of the polymers investigated in the presented study. We emphasize that the spectra of the polymers cannot be fit by a Cole−Davidson distribution. It appears that two parameters α and β (as in the case of the GGE distribution) are needed to take into account the overall width (α) and high-frequency exponent (β) of the distribution of the α-peak, a feature also observed in the spectra of simple glass formers.[21,22] In addition, two parameters appear for describing the excess wing, namely, its exponent γ and the onset of the wing σ. Usually the parameter α is determined for a spectrum which resolves the α-peak best and then is kept constant for all other temperatures. We emphasize that the results $T_g(M)$ do not depend on the particularly applied fit of the dielectric spectra which was checked by comparing the result for $T_g(M)$ with those from simple "peak picking", i.e., defining via $\tau_\alpha(T) = 1/(2\pi\nu_{peak})$.

In most of the polystyrene samples a more or less pronounced DC conductivity contribution is observed in the imaginary part of $\varepsilon(\omega)$ (cf. section 5), which is removed by subtracting the expression[23]

$$\varepsilon''_{DC} = \frac{\sigma_{DC}}{\varepsilon_0 \omega^a} \tag{1}$$

from the overall dielectric spectra. The exponent a turns out to be very close to 1. The time constants $\tau_\alpha(T)$ of the main relaxation (α-process) were interpolated or in a few cases extrapolated by applying the Vogel−Fulcher−Tammann (VFT) equation, explicitly

$$\lg\frac{\tau_\alpha}{\tau_0} = \frac{D}{T - T_0} \tag{2}$$

As first systematically applied by Stickel et al.,[24] the VFT equation can be linearized if the quantity S is derived from the data, specifically

$$S(T) = \left(\frac{-\mathrm{d}\lg\tau_\alpha}{\mathrm{d}T}\right)^{-1/2} = D^{-1/2}(T - T_0) \tag{3}$$

This expression will be used to extract the parameters D and T_0.

3. Results

A. Dielectric Spectra of Polydimethylsiloxane (PDMS). As an example, Figure 1a shows dielectric spectra of PDMS21600. In addition to the α-peak shifting with temperature, one observes an excess high-frequency contribution which is usually just called the excess wing.[21,22,25,26] The spectra can be well interpolated by an extension of the generalized gamma distribution (GGE distribution[21,22]) including both the α-peak (parameters α and β) and the excess wing (exponent γ and σ) as demonstrated in Figure 1a. A Cole−Davidson distribution does not work. In the case of simple glass formers such as glycerol[22] the value α may take values of 10−20, whereas for PDMS one finds $\alpha = 1.4$ (independent of M), indicating that the α-peak is very broad, and γ is found to lie in the range 0.1−0.18. We emphasize that the low-frequency part ($\omega\tau_\alpha \ll 1$) is well interpolated by the GGE function, demonstrating that here the Debye limit, $\varepsilon'' \propto \nu^1$, is reached. Thus, in this respect the dielectric relaxation spectra of type B polymers are just like

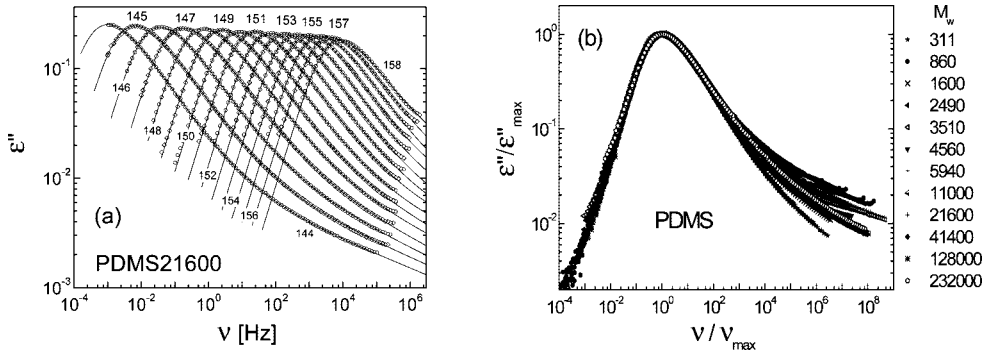

Figure 1. (a) Dielectric spectra for PDMS with $M_w = 21\,600$ g/mol for temperatures as indicated, interpolation applying an extension of the gamma distribution (GGE); (b) master curves for each M (as indicated) obtained by collapsing spectra from different temperatures.

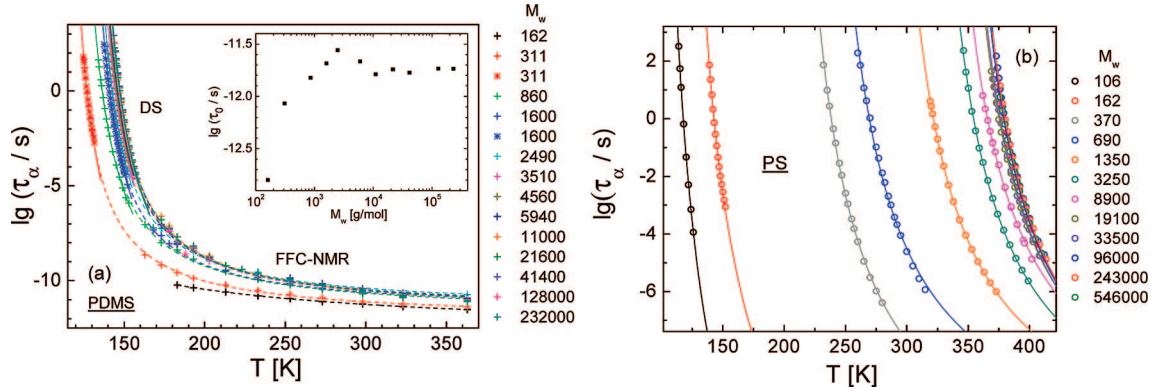

Figure 2. (a) Time constants $\tau_\alpha(T)$ extracted from the dielectric spectra (low-temperature data) and fast field cycling (FFC) NMR[27] (high-temperature data) of polydimethylsiloxane (PDMS); interpolation of all data applying the VFT equation with a single-parameter set (dashed lines) and interpolation of dielectric data only (solid line); (inset) exponential prefactor τ_0 of the VFT equation as a function of M; (b) polystyrene (PS); data interpolated by the VFT equation (solid lines).

those of a simple liquid, and applying, e.g., a Havriliak−Negami distribution, as often done, may be misleading as it often yields an unphysical exponent being smaller than 1 for the low-frequency side of the relaxation peak.

Figure 1b shows the spectra rescaled by their maximum height ε''_{max} and maximum frequency ν_{max}. Clearly, master curves are obtained from each set of spectra for a given M at the various temperatures. Except for the highest frequencies, for which some excess wing contribution manifests itself with different amplitude for different M in a nonsystematic way, the spectra coincide very well. A weak secondary relaxation peak (β-process) is observed only for PDMS860. We conclude that in the case of PDMS the spectral shapes of the segmental respectively glassy dynamics (α-process) are T as well as M independent, i.e., frequency temperature superposition (FTS) holds. The time constants $\tau_\alpha(T)$ obtained from the individual fits with the GGE distribution are shown in Figure 2a, and they will be used below for determining $T_g(M)$ (cf. section C). We note that the sample PDMS311 as well as PDMS1600 were measured twice because the temperature range possible to cover is very small (8 K) due to crystallization.

B. Dielectric Spectra of Polystyrene (PS). Figure 3 shows some examples of the dielectric spectra of polystyrenes with different molecular weights for which the conductivity (DC) contribution was removed by applying eq 1. In the Appendix (section 5) (Figure 17) we display the corresponding spectra as measured, i.e., with the DC contribution. As compared to PDMS the dielectric loss is significantly weaker and in the majority of samples the DC contribution varies significantly in strength; in some cases it is not at all discernible (cf. Figure 3b). For some samples the temperature dependence of the DC contribution scales with that of the α-process and for others not. Therefore, close to T_g it may happen that the α-peak gets almost hidden below a large DC contribution. Though the relaxation maximum is always resolved and allows for determining the relaxation time $\tau_\alpha(T)$, in some cases at very low frequencies ($\omega\tau_\alpha \ll 1$), spectral features such as a more or less pronounced shoulder or even a peak are discovered which cannot easily be attributed to some properly defined relaxation processes (Figure 3b). On the other hand, there are examples for which in the low-frequency limit the spectra as for PDMS exhibit a well-defined Debye limit (Figure 3c and 3d). The high-frequency part of the spectra shows the typical feature of an excess wing; however, in a few cases traces of a β-process are also recognized (cf. Figure 3a). Concerning all the mentioned spectral particularities no systematic relationship with molecular weight is discernible.

Figure 4 presents the dielectric spectra for different molecular weights and different temperatures scaled by ε''_{max} and plotted versus the reduced frequency $2\pi\nu\tau_\alpha$; here, the low frequency particularities found in some polystyrenes have been omitted. For a given PS sample FTS holds fairly well at least around the relaxation peak, however, the high frequency behavior is significantly different among the polystyrenes. Whereas the overall relaxation width is narrow and not much changing for the low M systems, a much broader relaxation peak is observed for $M \geq 690$ which is not much changing with M, *i.e.*, presumably at least for the latter polymers the α-relaxation is essentially independent of molecular weight. Whether the different behavior at high frequencies may be traced back to a different width of the α-peak itself or to quite different amplitudes of the excess wing cannot be decided. In any case the spectra can be well interpolated including α-peak and excess wing again by the GGE distribution (cf. Figure 3). The

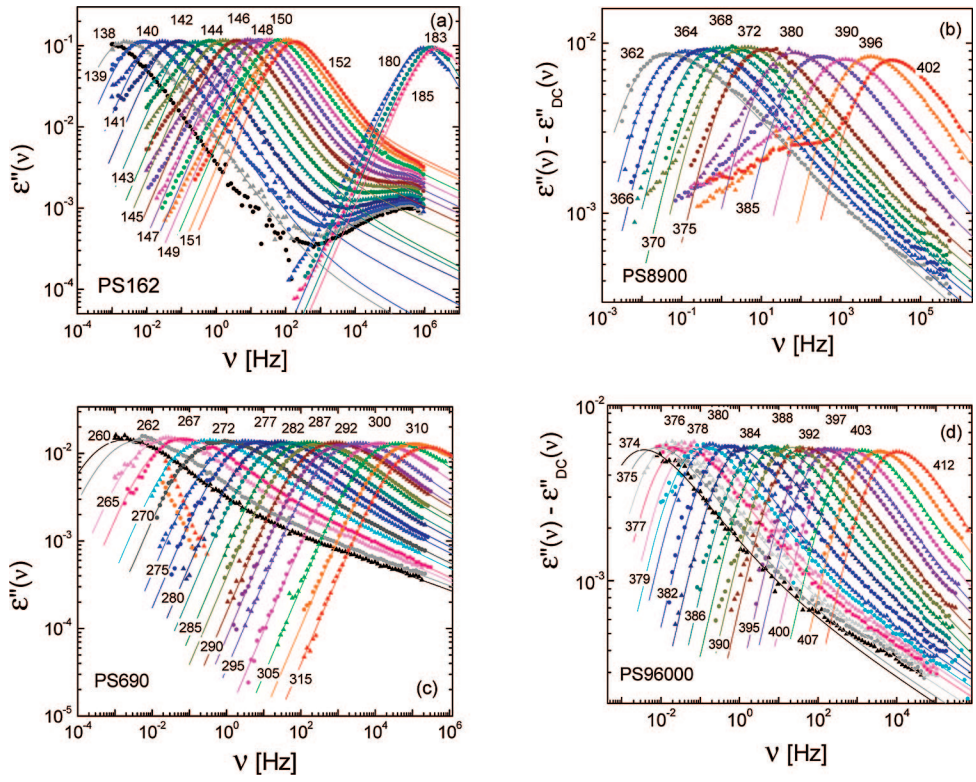

Figure 3. Examples of dielectric spectra of polystyrenes (PS) with different molecular weight M and interpolation by an extension of the generalized gamma distribution (solid lines). In the case of PS8900 and PS96000 the conductivity contribution was subtracted; in (a) the gap in the temperature range covered is due to crystallization.

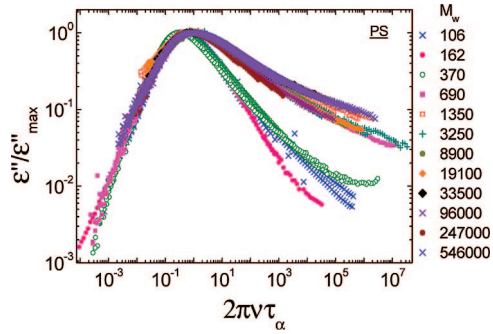

Figure 4. Master curves for each M (as indicated) obtained by collapsing the dielectric spectra of polystyrene (PS) from different temperatures.

corresponding time constants $\tau_\alpha(T)$ are displayed in Figure 2b. Whereas for PDMS the change of τ_α with M is weak (Figure 2a), in the case of PS a very strong change is observed. As will be shown below, T_g changes by more than 250 K for PS going from the monomeric glass former ethyl benzene to the high M limit.

C. Determining the Glass-Transition Temperature T_g. Defining T_g as the temperature at which the relaxation time is $\tau_\alpha = 100$ s, we applied the VFT equation (eq 2) to interpolate (or extrapolate in few cases) the $\tau_\alpha(T)$ data (cf. Figure 2). We display $T_g(M)$ for PB, PDMS, and PS in Figures 5a−7a. We note again that the dielectric spectra and corresponding time constants of PB are reported in ref 6. The so extracted $T_g(M)$ values are determined with an accuracy of ±0.2 K for PDMS, ±1.0 K for PS, and ±0.5 K for PB, i.e., the error bars in the figures are smaller than symbols. Any scatter must originate from a different source. Tentatively, the $T_g(M)$ traces are interpolated linearly by assuming three distinct regimes. The

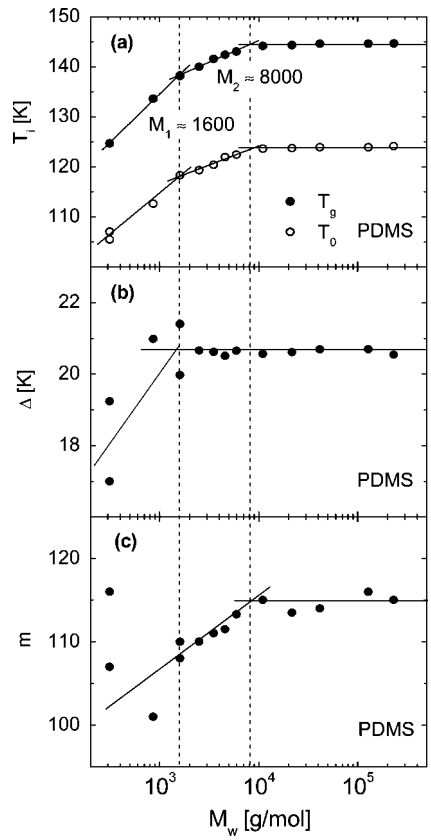

Figure 5. (a) $T_g(M)$ and $T_0(M)$ of the VFT equation for polydimethylsiloxane (PDMS), (b) difference $\Delta(M) = T_g - T_0$, and (c) fragility $m(M)$ as a function of molecular weight M: (solid lines) guide to the eye. Crossover molecular weights M_1 and M_2 are indicated by dashed lines.

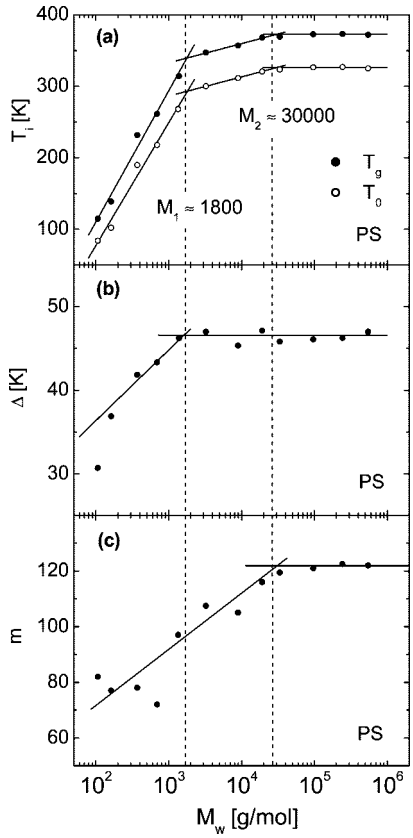

Figure 6. (a) $T_g(M)$ and $T_0(M)$ of the VFT equation for polystyrene (PS), (b) difference $\Delta(M) = T_g - T_0$, and (c) fragility $m(M)$ as a function of molecular weight M: (solid lines) guide to the eye. Crossover molecular weights M_1 and M_2 are indicated by dashed lines.

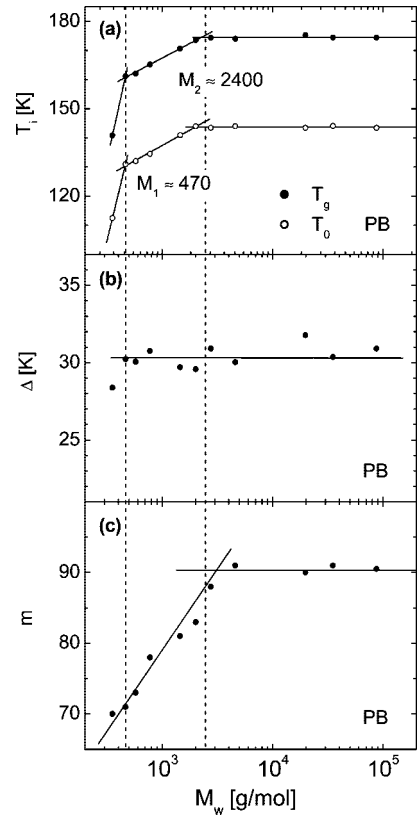

Figure 7. (a) $T_g(M)$ and $T_0(M)$ of the VFT equation for polybutadiene (PB), (b) difference $\Delta(M) = T_g - T_0$, and (c) fragility $m(M)$ as a function of molecular weight M: (solid lines) guide to the eye. Crossover molecular weights M_1 and M_2 are indicated by dashed lines.

justification of this and meaning of the crossover molecular weights M_1 and M_2 will become clear in due course. In section F the results for $T_g(M)$ will be compared to those of previous studies.

D. Determining the VFT Parameters. We applied the VFT equation (eq 2) for assessing the non-Arrhenius character of the temperature dependence of the time constants $\tau_\alpha(T)$. As seen in Figure 2, the time constants of the different polymers were compiled for quite different intervals of temperature and time scales and the number of points in the chart $\tau_\alpha(T)$ varies. Any standard VFT fitting procedure would thus provide parameters which cannot easily be compared among each other. In order to obtain reliable data for the VFT parameters $T_0(M)$ and $D(M)$ we applied the "Stickel method"[24] by linearizing the temperature derivative of the lg $\tau_\alpha(T)$, i.e., the quantity $S(T)$ is analyzed (cf. eq 3). The data $S(T)$ for PDMS are shown in Figure 8a. For all samples $S(T)$ is reproduced by a linear function. In other words, the VFT equation works well in the temperature range investigated. Only very few data points had to be discarded (in brackets). The parameter D which controls the slope of $S(T)$ appears virtually not to change with M. Similarly, for the case of PS, the quantity S is displayed as a function of $T - T_0$ (cf. Figure 8b). In this case a master curve is found. Similar results are also found for PB. For all three polymers D does not depend on M even down to the lowest M. For comparison we made individual fits of $S(T)$, and the corresponding $D(M)$ is displayed in Figure 9. Again, no trend is found for $D(M)$, though some scatter is recognized.

Given the scatter of $D(M)$ obtained by the individual fits, the most reliable way of extracting parameters D and $T_0(M)$ is from constructing master curves of the type shown in Figure 8b, and the mean values for D are 346 K for PDMS, 670 K for PS, and 428 K for PB. The corresponding T_0 values are included in Figures 5a−7a. It appears that the difference $\Delta(M) = T_g - T_0$ is constant, and thus, the same M dependence as for $T_g(M)$ may be anticipated also for T_0. However, a subtle change for low M values is recognized. There is a trend that $\Delta(M)$ becomes smaller at lowest M, best seen for PS for which the difference $\Delta(M)$ is largest and very low M systems were studied (cf. Figures 5b−7b). This effect sets in only below $M \cong 1500$ for PS and even lower for PDMS and PB and thus may be close to the crossover at M_1 as found for the $T_g(M)$ behavior in Figures 5a−7a.

Regarding the exponential prefactor τ_0, it becomes M dependent only at lowest M, say below M_1. This becomes obvious when inspecting $\tau_0(M)$ for PDMS in the inset of Figure 2a. At $M < 1000$ the prefactor τ_0 decreases, which is also directly seen when NMR data[27] are included for $\tau_\alpha(T)$ in Figure 2a. This feature is also observed for PS (cf. Figure 11).

E. Determining Fragility. The concept of fragility is around in glass science since long, and numerous publications attempt to install some relationship between fragility and structural as well as dynamical properties of different glass formers. One way of measuring fragility is given by determining the fragility index m, explicitly

$$m = -\left.\frac{d \lg \tau_\alpha(T/T_g)}{d(T/T_g)}\right|_{T_g} = T_g(M)\frac{D}{\Delta(M)^2} = T_g(M)F(M) \quad (4)$$

In the second part of the equation m is expressed in terms of the VFT equation (eq 2), and the quantity F denotes the temperature derivative of lg $\tau_\alpha(T)$ at T_g. As in the case of the parameters of the VFT equation most of the m values published scatter strongly and may show systematic errors. In order to get reliable and comparable results for the series of polymers

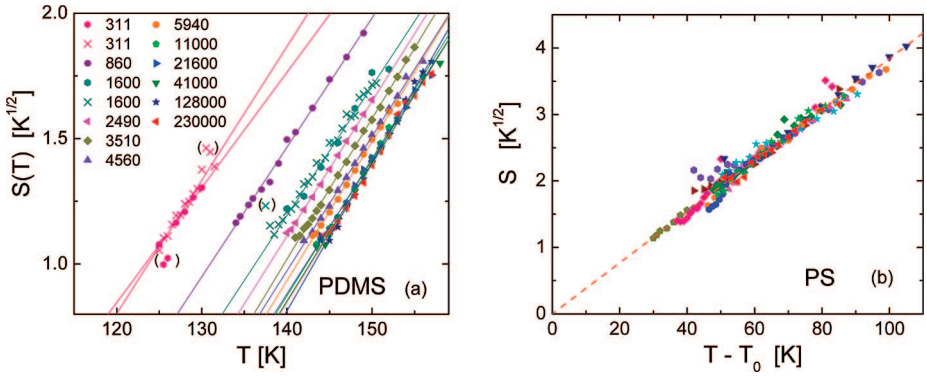

Figure 8. Linearizing the VFT equation by applying the derivative method. (a) The quantity $S(T)$ as defined in eq 3 is plotted for the series of polydimethylsiloxane (PDMS): (straight lines) linear interpolations. (b) Master curve for S as a function of $T - T_0$ for the series of polystyrenes (PS): (straight line) linear interpolation.

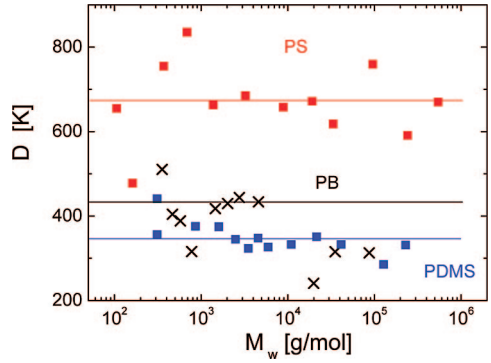

Figure 9. Parameter D of the VFT equation derived from individual fits to $S(T)$ (cf. eq 2) as a function of molecular weight M for the series of PDMS, PS, and PB; lines indicate D values obtained from master curves as shown in Figure 8b.

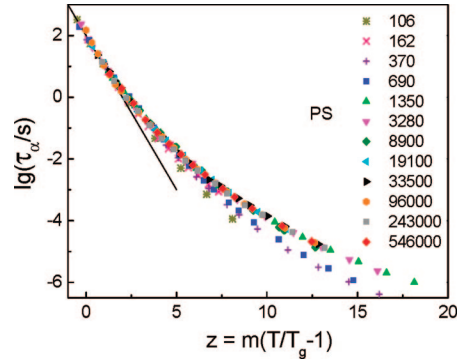

Figure 11. Master curve for the segmental relaxation time τ_α of polystyrene (PS) in order to determine the fragility $m(M)$ (cf. Figure 6c). The data are displayed as a function of the reduced variable z, cf. eq 5: (solid line) fixing the absolute value to 2 and slope to -1 at T_g.

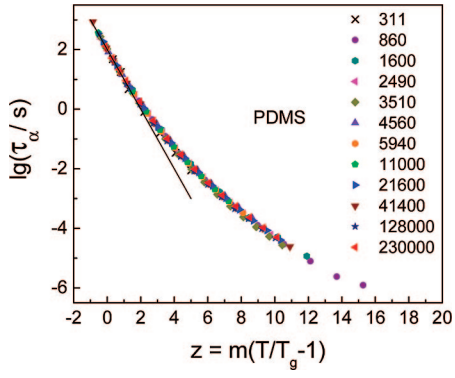

Figure 10. Master curve for the segmental relaxation time τ_α for polydimethylsiloxane (PDMS) in order to determine the fragility $m(M)$ (cf. Figure 5c). The data are displayed as a function of the reduced variable z, cf. eq 5: (solid line) fixing the absolute value to 2 and slope to -1 at T_g.

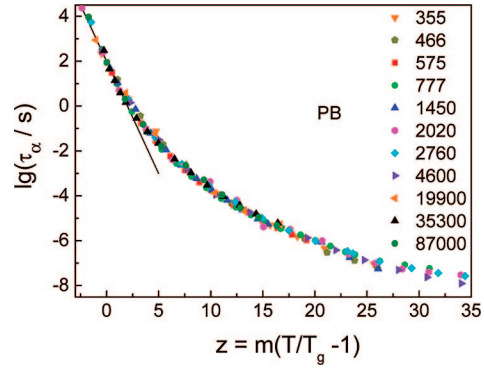

Figure 12. Master curve for the segmental relaxation time τ_α of polybutadiene (PB) in order to determine the fragility $m(M)$ (cf. Figure 7c). The data are displayed as a function of the reduced variable z, cf. eq 5: (solid line) fixing the absolute value to 2 and slope to -1 at T_g.

under investigation we cast the VFT equation in a form containing the parameters m and T_g instead of T_0 and D. As shown, e.g., by Blochowicz et al.,[22] one can write

$$\lg\left(\frac{\tau_\alpha}{\tau_0}\right) = \frac{K_0^2}{m(T/T_g - 1) + K_0} \quad \text{with} \quad K_0 = \lg\left(\frac{\tau_g}{\tau_0}\right) \tag{5}$$

Here, the quantity τ_g is the relaxation time at T_g (according to our definition of T_g, we set $\tau_g = 100$ s) and τ_0 is the exponential prefactor. If we plot lg τ_α as a function of the quantity $m(T/T_g - 1)$, the resulting curves coincide at T_g and have the same derivative at T_g. If in addition the corresponding τ_0 are similar one gets even a master curve as long as the VFT equation applies. A significantly different τ_0 would show up in a spread of the curves at high temperatures only. We show the rescaled data for PDMS, PS, and PB in Figures 10, 11, and 12, respectively. Here, m was determined in such a way to get the best agreement with a straight line fixing the absolute value to 2 and slope to -1 at T_g. In all cases very good master curves are obtained even up to the highest temperatures, indicating that the prefactor τ_0 essentially does not change with M for a given polymer series. As already discussed (cf. Figure 2a) a trend for a somewhat lower τ_0 value is recognized at lowest M, best seen for PS, for which the three samples with the lowest M deviate somewhat from the master curve. Thus, for determining the VFT

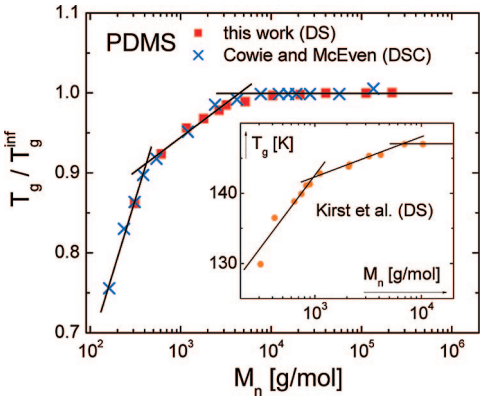

Figure 13. Comparison of $T_g(M)$ results from different studies on polydimethylsiloxane (PDMS): DS, dielectric spectroscopy; DSC, differential scanning calorimetry. Solid lines represent linear interpolation assuming three distinct regimes.

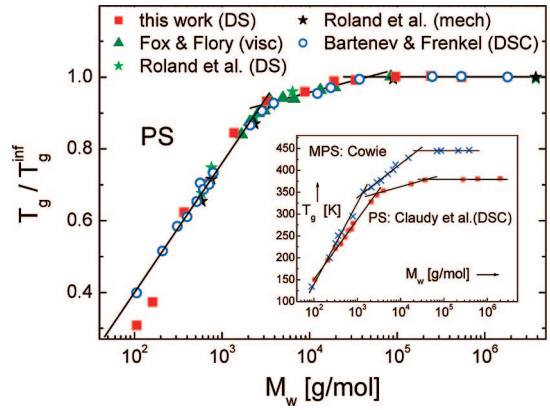

Figure 14. Comparison of $T_g(M)$ results from different studies of polystyrene (PS): DS, dielectric spectroscopy; DSC, differential scanning calorimetry; mech, mechanical relaxation; visc, viscosity. (Inset) Additional data for PS and poly(α-methylstyrene) (MPS). Solid lines represent linear interpolation assuming three distinct regimes.

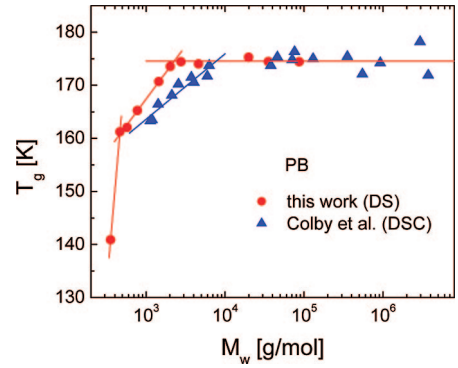

Figure 15. Comparison of $T_g(M)$ results from different studies of polybutadiene (PB): DS, dielectric spectroscopy; DSC, differential scanning calorimetry.[33] Solid lines represent linear interpolation assuming three distinct regimes.

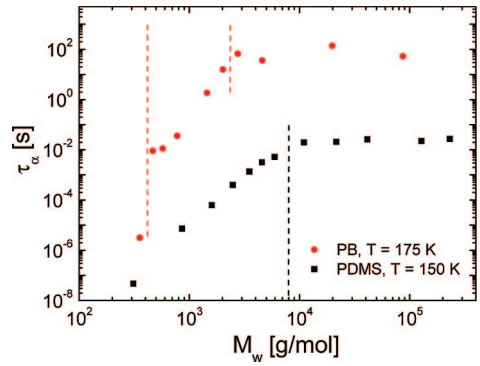

Figure 16. Time constant $\tau_\alpha(M)$ of the α-process ("segmental" relaxation) for PB and PDMS as a function of molecular weight M at constant temperature; straight lines indicate crossover molecular weights (cf. Figure 2a).

parameters in the full M range, it is not possible to fix τ_0 as sometimes done in the literature.

Inspecting the corresponding results for $m(M)$ displayed in Figures 5c−7c one recognizes for polymers a well-defined crossover from m increasing with M at low M to m = constant at high M. Comparing the crossover molecular weights with those of $T_g(M)$ from Figures 5a−7a the values are very close to M_2. In other words, $T_g(M)$ as well as $m(M)$ saturate only above M_2 whereas below a pronounced M dependence can be found. Vice versa, we take the appearance of a noncontinuous behavior of $m(M)$ as a further justification to discriminate distinct regimes in $T_g(M)$.

Here, the question arises why in $m(M)$ only one kink appears at M_2 whereas the $T_g(M)$ data suggest two kinks at M_1 and M_2. According to eq 4 m depends not only on T_g but also on the difference $\Delta(M) = T_g - T_0$. As shown in Figures 5b−7b above M_1 the difference $\Delta(M)$ is constant. Thus, here the fragility m is proportional to $T_g(M)$ and reflects the M dependence of the latter. However, below M_1 the difference $\Delta(M)$ decreases with lowering M. According eq 4 this will attenuate the effect of the rather strong dependence of $T_g(M)$ at lowest M. This explains why the first crossover molecular weight M_1 does not show up in $m(M)$.

F. Comparison with Previous Results for $T_g(M)$. The glass transition of the polymers PDMS, PS, and PB was already investigated as a function of M by many techniques in the majority of cases by means of DSC and mechanical and dielectric (DS) relaxation experiments. In most cases the absolute values of $T_g(M)$ disagree slightly, however, the qualitative trend is very similar. For allowing a quantitative comparison we plot the ratio $T_g(M)/T_g^{inf}$ where T_g^{inf} denotes the saturation value of T_g at highest M. In Figure 13 we compare the DSC data of Cowie and McEven[28] for PDMS with those from the present dielectric study as a function of the number-average molecular weight M_n (Cowie and McEven reported only M_n). The agreement is very good, and a linear interpolation assuming three distinct regimes is even more convincing as the DSC data for PDMS were investigated down to somewhat lower M_n than in our DS study. No systematic differences are observed between the results of the two techniques, though they are probing the glass transition via quite different quantities. We note that displaying the data as a function of M_n leads to different crossover molecular weights M_1 as polydispersity cannot be completely ignored for the low M PDMS samples (cf. Table 1). The dielectric data of Kirst et al.[29] exhibit larger scatter and do not cover sufficiently high M needed for a full comparison, yet linear interpolations with similar crossover molecular weights are possible (cf. inset Figure 13). Again, different polydispersity as well as different end groups become influential at low M, and this may explain the somewhat different crossover molecular weights M_1 observed for the Kirst et al. data compared to our results.

In the case of polystyrene (PS) we compare our data with the DSC results from and Bartenev and Frenkel,[8] cf. Figure 14. These authors also linearly interpolated their data in three regimes. In addition, we added the results from a viscosity study by Fox and Flory[30] and a dielectric as well as mechanical relaxation study by Roland and co-workers.[12,31] Again, the data agree well and justify a noncontinuous interpolation including

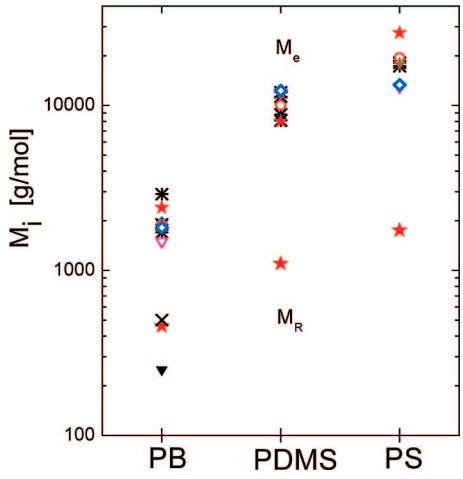

Figure 17. Data for entanglement molecular weight M_e for PB,[37−41] PDMS,[37−39,41,42] and PS[37−39,41,43] and Rouse unit weight M_R for PB[5,33] as reported in the literature. The (red) stars show M_e and M_R estimated from the present $T_g(M)$ study.

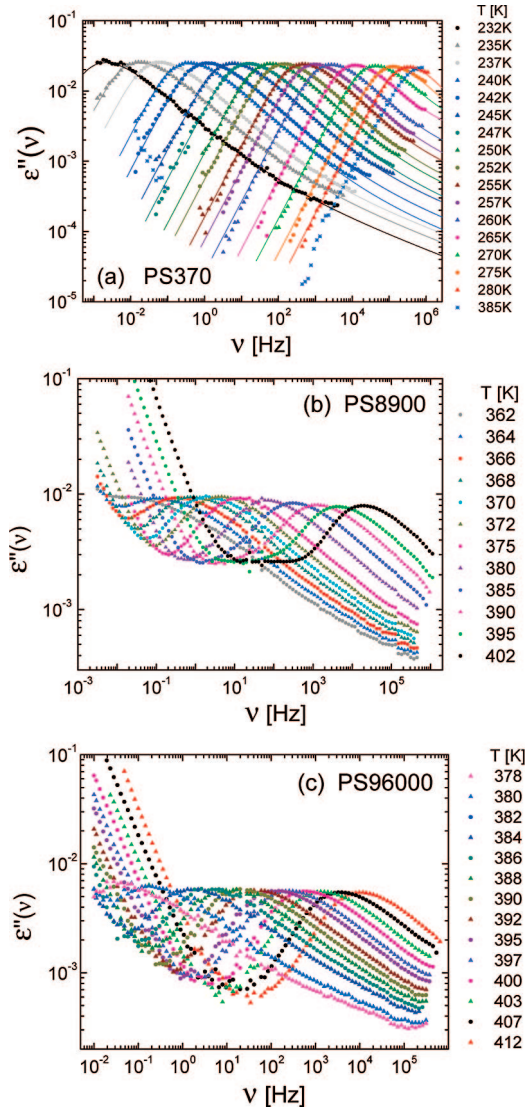

Figure 18. Examples of dielectric spectra of polystyrene (PS) with different molecular weight M as indicated with varying strength of conductivity contribution.

all the mentioned $T_g(M)$ results. Claudy et al.[32] reported from DSC $T_g(M)$ containing monodisperse PS oligomers up to PS_7, and the data are displayed in the inset of Figure 14. Again, three regimes can be easily recognized with crossover molecular weights being close to those of the present study. The T_g values of the two lowest M polystyrenes of the present study deviate a little from the results of the other PS studies. At such low M one has to keep in mind that the end groups stemming from the initializer used for anionic polymerization may play a role. In the case of our PS *sec*-butyllithium was taken, i.e., a hexyl group is attached to the benzene ring in the PS160 sample. Moreover, for the lowest M Claudy et al. measured styrene, whereas the present study chose ethyl benzene. For the bi- and tristyrene Claudy et al. measured 2,4-diphenyl-1-butene and 2,4,6-triphenyl-1-hexene, respectively. In the case of the data of Bartenev and Frenkel, no such information is available. Finally, we add the $T_g(M)$ data for poly(α-methylstyrene) (MPS) from Cowie,[10] which show quite similar behavior, again allowing discriminating three regimes (cf. Figure 14 inset).

The situation for 1,4-polybutadiene (PB) is less satisfactory.To our knowledge only a single systematic DSC study was carried out by Colby et al.[33] In Figure 15 at high M the DSC data agree well with the present ones even on an absolute scale, though strong scatter is observed for the DSC results. A clear-cut crossover to a strong M dependence is observed below ca. $M_w \cong 7000$, which is a factor of about 3 higher than in the present DS data. No data are reported in the low M limit by Colby et al. Few polybutadiene samples were also measured by Kisliuk et al.[15] and show again a saturation of $T_g(M)$ only above $M \cong 7000$. We attribute this difference to a different microstructure of PB samples. The vinyl content in the latter two studies was always below 10%, whereas in our case we determined via high-resolution ^{13}C NMR a vinyl content changing from 20% at low M to 6−8% at high M.[19] It is well known that the microstructure of PB has a pronounced influence on the dynamics.[34] The slight trend in $D(M)$ observed in Figure 9 may also be attributed to this changing microstructure.

4. Discussion and Conclusions

We reported dielectric (DS) spectra of a series of PDMS, PS, and PB samples with different molecular weights including very low M values. No systematic spectral changes are observed in the line shape of the main relaxation peak as a function of molecular weight. In particular, in PDMS the shape of the α-peak is M and T independent, in very good approximation. Similar results were also reported by other studies, though not always including the low M limit.[12,31] Differences appearing at high frequencies attributed to secondary relaxation processes as well as the magnitude of the DC contribution at low frequency do not show any systematic trend with M. The $T_g(M)$ as well as $T_0(M)$ values obtained from analyzing DS spectra may in all cases be interpolated by assuming three distinct regimes. Comparing our results with literature data, they agree well in particular with those from Cowie and McEven (PDMS),[28] Bartenov and Frenkel (PS),[8] and Claudy et al. (PS),[32] who covered a sufficiently broad M range and also reported non-continuous $T_g(M)$ curves. We mention that in a viscosity (η) study of low molecular weight PS Gray et al.[35] reported two kinks in the function $\eta(M)$. Specifically, for a given temperature, in addition to the kink at the entanglement molecular weight M_c a marked fall in viscosity was observed below $M = 1100$, which was attributed to the presence of a nonpolymeric liquid. Displaying our data on PB as well as on PDMS together with results from a field cycling NMR study[27] (cf. Figure 2a) in the same way, we present $\tau_\alpha(M)$ for a single temperature in Figure 16. Again, a clear-cut change is observed at M_2, and it is more pronounced than in $T_g(M)$. The change at M_1 is less obvious for PDMS as high-temperature data is missing for the sample with lowest M. Although quite different physical quantities,

namely, viscosity η vs segmental time constant τ_α, are considered, both appear to reflect the emergence of specific polymer dynamics. We conclude that both the data sets for $T_g(M)$ and $\tau_\alpha(M)$ discussed here give a hint that indeed a noncontinuous M dependence revealing two crossover molecular weights M_1 and M_2 may be more adequate than a continuous one, as suggested by free-volume theories, and thus, we reconfirm the results by Cowie and co-workers.

Regarding the VFT parameter D it is found to be M independent within the accuracy of the experiments for all three polymers, and T_0 essentially follows $T_g(M)$. Here, we emphasize that in most reports $D(M)$ (as well as $m(M)$) suffers from strong scatter, which does not allow for any definite conclusion. We think applying the "Stickel method", as done in the present contribution, yields more reliable $D(M)$ values. Given that D and $\Delta(M) = T_g - T_0$ are independent of M (above M_1, cf. Figures 13c−15c), this is compatible with the segmental time constant being the same function of $T - T_g$ independent of M as already found, e.g., by Plazek and O'Rourke.[36] In other words, the quantity F in eq 5 is constant at $M > M_1$. Below M_1 the difference $\Delta(M)$ shows a weak though recognizable trend to become smaller for decreasing M.

Determining reliable fragility values $m(M)$ by constructing a master curve for τ_α by scaling out T_g as well as m, only a single kink appears at M_2 which can be explained when the VFT eq 2 is inspected. Here, the crucial point is the behavior of $\Delta(M) = T_g - T_0$ which, as just mentioned, increases with M in the simple liquid regime at $M < M_1$ but saturates already at M_1, that is, the behavior of $m(M)$ follows that of $T_g(M)$ in the regime $M > M_1$ but the strong increase of $T_g(M)$ at very low $M < M_1$ is effectively compensated by the factor $1/\Delta(M)^2$ in eq 4. We cannot confirm reports stating that fragility is independent of M.[12,14,17,18] Yet, in the case of PDMS the change of $m(M)$ is rather small as is $T_g(M)$ and may easily be overlooked. Moreover, as the shape of the main relaxation peak is virtually independent of M but fragility changes significantly the polymers studied here do not support the claim that fragility and stretching are correlated. The quantity F turns out to be M independent for $M > M_1$ and is connected to the fragility by $m = FT_g$ (eq 4). In other words, the mere definition of fragility via the "fragility plot" $\tau_\alpha(T_g/T)$ or $\tau_\alpha(T/T_g)$ introduces the M dependence of fragility for polymers ($M > M_1$). We note that Qin and McKenna[16] reported a correlation of m and T_g for several types of glass formers, which was later challenged by Sokolov et al.[18]

Summarizing the M dependence of the glass transition as reflected in the parameters of interpolating $\tau_\alpha(T)$ it turns out that not only $T_g(M)$ but also $\Delta(M)$ as well as $m(M)$ show particularities which cannot easily be explained by common wisdom. All together, they point to a noncontinuous M dependence of the glass-transition phenomenon in polymers, in any case to a situation which deserves to be revisited.

Given the $T_g(M)$ results of the present study as well as further indications in the literature it is indeed possible that $T_g(M)$ reflects changes of polymer dynamics. In contrast to common belief, it is tempting to attribute M_1 to the Rouse unit M_R and M_2 to the entanglement molecular weight M_e. In Figure 17 we compiled literature data for M_e and included the M_2 values (large stars) obtained from our $T_g(M)$ curves. We used the following references for PDMS,[37−39,42] PS,[37−39,41,43] and PB.[37−41] The results agree within the uncertainties given by the different techniques determining M_e. This we take as a strong hint that actually a second kink exists in $T_g(M)$ and that it reflects M_e at which entanglement starts in the polymer melt. Regarding the first kink observed for $T_g(M)$ at M_1, we attribute it to the Rouse unit M_R as done in our recent field cycling NMR study.[5] However, literature data for M_R is rare. For PB we included results from our FCC NMR[5] and ^{2}H NMR[44] studies finding a fair agreement. Thus, it is possible that the different dynamic regimes discussed for polymers are also reflected in $T_g(M)$ (as well as in $m(M)$), namely, simple liquid (glassy) dynamics ($M < M_R$), Rouse ($M_R < M < M_e$), and entanglement dynamics ($M > M_e$). Of course, more experiments including in particular very low M "polymers" have to be carried out in order to finally settle this question.

There is no polymer and glass theory that predicts such a connection of polymer and glassy behavior. As polymer dynamics and glassy dynamics are believed to involve quite different length and time scales it is natural to assume mutual independence. Here, we want to draw the attention to our recent results regarding the segmental correlation function $F_2(t)$ studied by fast field cycling (FFC) NMR.[5,6] Covering a broad frequency and temperature range for PB, we were able to study the region of both glassy dynamics as well as polymer dynamics. According to this analysis, the segmental correlation function can be decomposed into two parts, namely, glassy dynamics ($\phi_{glass}(t)$) and polymer dynamics ($F_{polymer}(t)$) (cf. also ref 45), explicitly we write

$$F_2(t) = \lfloor (1-f)\phi_{glass}(t) + f \rfloor F_{polymer}(t) \quad (6)$$

At $M > M_R$, in the course of establishing Rouse modes in the polymer melt the relaxation strength $1 - f$ of the glassy dynamics decreases successively until it stays essentially constant when entanglement sets in. In other words, the fraction of correlation decaying via the glassy dynamics decreases, i.e., the segmental reorientations, become more and more spatially restricted due to the emergence of Rouse dynamics. We note that f is on the order of 0.1 for high M polybutadiene, and it is related to what has been called the dynamic order parameter $S = f^{1/2}$.[6,46] Thus, already in the Rouse regime polymer dynamics impede the segmental dynamics governed by the glass transition. This redistribution of glassy and polymer relaxation is not yet properly understood,[47] but it may well be possible that also the time constants $\tau_\alpha(T)$ and $\tau_\alpha(M)$ are modified due to this mechanism.

5. Appendix

Figure 18 shows examples of dielectric spectra with different strength of conductivity (DC) contribution. In Figure 3, the DC contribution has been subtracted according to eq 1.

Acknowledgment. Helpful discussions with V. N. Novikov (Novosibirsk) and A. H. E. Müller (Bayreuth) and the financial support through Deutsche Forschungsgemeinschaft (SFB 481 and RO 907/10) are appreciated.

References and Notes

(1) Ding, Y.; Kisliuk, A.; Sokolov, A. P. *Macromolecules* **2004**, *37*, 161–166.
(2) Jacobsson, P.; Börjesson, L.; Torell, L. M. *J. Non-Cryst. Solids* **1991**, *131−133*, 104–108.
(3) Doi, M.; Edwards, S. F. *The Theory of Polymer Dynamics*; Oxford Scientific Publications: New York, 1986.
(4) Fox, T.; Flory, P. J. *J. Polym. Sci.* **1954**, *14*, 315–319.
(5) Kariyo, S.; Gainaru, C.; Schick, H.; Brodin, A.; Novikov, V. N.; Rössler, E. A. *Phys. Rev. Lett.* **2006**, *97*, 2078031−207803-4. (a) Erratum: Kariyo, S.; Herrmann, A.; Gainaru, C.; Schick, H.; Brodin, A.; Novikov, V. N.; Rössler, E. A. *Phys. Rev. Lett.* **2008**, *100*, 109901–1.
(6) Kariyo, S.; Herrmann, A.; Hintermeyer, J.; Gainaru, C.; Schick, H.; Brodin, A.; Novikov, V. N.; Rössler, E. A. *Macromolecules* **2008**, *41*, 5322–5332.
(7) Cowie, J. M. G. *Eur. Polym. J.* **1975**, *11*, 297–300.
(8) Bartenev, G. M.; Frenkel, S. Ya. *Polymer Physics*; Khimija: St. Petersburg, 1990.
(9) Cowie, J. M. G. *Chemie und Physik der Polymeren*, 1st ed.; Verl. Chemie: Weinheim, 1976.
(10) Cowie, J. M. G.; Arrighi, V. *Polymers: Chemistry and Physics of Modern Materials*, 3rd ed.; CRC Press: Boca Raton, 2008.

(11) Sperling, L. H. *Introduction to Physical Polymer Science*, 2nd ed.; John Wiley & Sons: New York, 1992.
(12) Sperling, L. H. *Introduction to Physical Polymer Science*, 3rd ed.; John Wiley & Sons: New York, 2001.
(13) Roland, C. M.; Ngai, K. L. *Macromolecules* **1996**, *29*, 5747–5750.
(14) Santangelo, P. G.; Roland, C. M. *Macromolecules* **1998**, *31*, 4581–4548.
(15) Kisliuk, A.; Ding, Y.; Hwang, J.; Lee, J. S.; Annis, B. K.; Foster, M. D.; Sokolov, A. P. *J. Polym. Sci. Polym. Phys.* **2002**, *40*, 2431–2439.
(16) Qin, Q.; McKenna, G. *J. Non-Cryst. Solids* **2006**, *352*, 2977–2985.
(17) Ding, Y.; Novikov, V. N.; Sokolov, A. P.; Cailliaux, A.; Dalle-Ferrier, C.; Alba-Simionesco, C.; Frick, B. *Macromolecules* **2004**, *37*, 9264–9272.
(18) Sokolov, A. P.; Novikov, V. N.; Ding, Y. *J. Phys.: Condens. Matter* **2007**, *19*, 205116-1–205116-8.
(19) Lusceac, S. A.; Gainaru, C.; Vogel, M.; Medick, P.; Koplin, C.; Rössler, E. A. *Macromolecules* **2005**, *38*, 5625–5633.
(20) Stockmayer, W. H. *Pure Appl. Chem.* **1967**, *15*, 539–554.
(21) Blochowicz, Th.; Tschirwitz, Ch.; Benkhof, St.; Rössler, E. A. *J. Chem. Phys.* **2003**, *118*, 7544–7555.
(22) Blochowicz, Th.; Gainaru, C.; Medick, P.; Tschirwitz, C.; Rössler, E. A. *J. Chem. Phys.* **2006**, *124*, 134503-1–134503-11.
(23) Böttcher, C. J. F.; Borderwijk, P. *Theory of Electric Polarization*, 2nd ed.; Elsevier: Amsterdam, 1978; Vol. 2.
(24) Stickel, F.; Fischer, E. W.; Richert, R. *J. Chem. Phys.* **1995**, *102*, 6251–6257.
(25) Lunkenheimer, P.; Schneider, U.; Brand, R.; Loidl, A. *Contemp. Phys.* **2000**, *41*, 15–36.
(26) Blochowicz, T.; Brodin, A.; Rössler, E. A. *Adv. Chem. Phys.* **2006**, *133*, 127–256.
(27) Herrmann, A.; Rössler, E. A. Unpublished results.
(28) Cowie, J. M. G.; McEven, I. *J. Polymer* **1973**, *14*, 423–426.
(29) Kirst, K. U.; Kremer, F.; Pakula, T.; Hollingshurst, J. *Colloid Polym. Sci.* **1994**, *272*, 1420–1429.
(30) Fox, T.; Flory, P. J. *J. Appl. Phys.* **1950**, *21*, 581–591.
(31) Roland, C. M.; Casalini, R. *J. Chem. Phys.* **2003**, *119*, 1838–1842.
(32) Claudy, P.; Létoffé, J. M.; Camberlain, Y.; Pascault, J. P. *Polym. Bull.* **1983**, *9*, 208–215.
(33) Colby, R. H.; Fetters, L. J.; Graessley, W. W. *Macromolecules* **1987**, *20*, 2226–2237.
(34) Zorn, R.; Mopsik, F. I.; McKenna, G. B.; Willner, L.; Richter, D. *J. Chem. Phys.* **1997**, *107*, 3645–3655.
(35) Gray, R. W.; Harrison, G.; Lamb, J. *Proc. R. Soc. London* **1977**, *356*, 77–102.
(36) Plazek, D. J.; O'Rourke, V. M. *J. Polym. Sci. Polym. Phys.* **1971**, *9*, 209–243.
(37) Ferry, J. D. *Viscoelastic Properties of Polymers*; Wiley: New York, 1980.
(38) Mark, J. E. *Physical Properties of Polymers Handbook*; Horwood: New York, 1996.
(39) Cahn, R. W.; Haasen, P.; Kramer, E. J. *Materials Science and Technology*; VHC: Weinheim, 1993; Vol. 12.
(40) Pearson, D. S.; Helfand, E. *Macromolecules* **1984**, *17*, 888–895.
(41) Fetters, L. J.; Lohse, D. J.; Richter, D.; Witten, T. A.; Zirkel, A. *Macromolecules* **1994**, *27*, 4639–4647.
(42) Appel, M.; Fleischer, G. *Macromolecules* **1993**, *26*, 5520–5525.
(43) Antonietti, M.; Coutandin, J.; Sillescu, H. *Macromolecules* **1986**, *19*, 793–798.
(44) Klein, P. G.; Adams, C. H.; Brereton, M. G.; Ries, M. E.; Nicholson, T. M.; Hutchings, L. R.; Richards, R. W. *Macromolecules* **1998**, *31*, 8871–8877.
(45) Kimmich, R.; Fatkullin, N. *Adv. Polym. Sci.* **2004**, *170*, 1–113.
(46) Dollase, T.; Graf, R.; Heuer, A.; Spiess, H. W. *Macromolecules* **2001**, *34*, 298–309.
(47) Brodin, A. *J. Chem. Phys.* **2008**, *128*, 104901-1–104901-8.

MA8016794